

Long term H-release of hard and intermediate between hard and soft amorphous carbon evidenced by in situ Raman microscopy under isothermal heating

C. Pardanaud^a, C. Martin^a, G. Giacometti^a, P. Roubin^a, B. Pégourie^b,
C. Hopf^c, T. Schwarz-Selinger^c, W. Jacob^c, J.G. Buijnsters^d

^aAix-Marseille Université, CNRS, PIIM UMR 7345, 13397 Marseille cedex 20, France.

^bCEA, IRFM, 13108 Saint-Paul-lez-Durance, France.

^cMax-Planck-Institut für Plasmaphysik, EURATOM Association, Boltzmannstr. 2, 85748 Garching, Germany.

^dDepartment MTM, Katholieke Universiteit Leuven, Kasteelpark Arenberg 44, B-3001 Leuven, Belgium.

Abstract

We study the kinetics of the H release from plasma-deposited hydrogenated amorphous carbon films under isothermal heating at 450, 500 and 600 °C for long times up to several days using in situ Raman microscopy. Four Raman parameters are analyzed. They allow the identification of different processes such as the carbon network reorganization and the H release from sp^3 or sp^2 carbon atoms and the corresponding timescales. Carbon reorganization with aromatization and loss of sp^3 hybridization occurs first in 100 minutes at 500 °C. The final organization is similar at all investigated temperatures. Full H release from sp^3 carbon occurs on a longer timescale of about 10 hours while H release from sp^2 carbon atoms is only partial, even after several days. All these processes occur more rapidly with higher initial H content, in agreement with what is known about the stability of these types of films. A quantitative analysis of these kinetics studies gives valuable information about the microscopic processes at the origin of the H release through the determination of activation energies.

Published in: Diamond and Related Materials, **37**, 92–96 (2013)
doi: 10.1016/j.diamond.2013.05.001

Submitted: 14.03.2013
Accepted: 07.05.2013
Available online 23.05.2013

1. Introduction

Raman spectroscopy is a powerful tool to rapidly characterize C-based materials that contain sp^2 carbon atoms ($C(sp^2)$). Interpreting the 1000 - 1800 cm^{-1} spectral region gives information on the carbon organization (aromatization). Because the Raman cross section for $C(sp^3)$ is one to two orders of magnitude lower than that of $C(sp^2)$, two bands due to $C(sp^2)$ dominate this spectral range even when samples contain only a few percent of $C(sp^2)$. They are the well-known G and D bands [1]. They contain information on disorder such as the size of aromatic domains, the $C(sp^2)/C(sp^3)$ ratio for amorphous carbons (a-C), and the H content for hydrogenated carbons (a-C:H) [1-3]. Raman parameters generally used to probe the bonding structure are: the width and the position of the G and D bands, denoted $\Gamma_{G,D}$ and $\sigma_{G,D}$ respectively, the height ratio of these two bands, H_D/H_G , and if applicable, the m/H_G parameter with m being the slope of the photoluminescence background calculated between 800 and 2000 cm^{-1} . In the case of heat-treated a-C:H films for which the H content varied from 2 to 30 at. %, we have recently obtained a linear relation between $\log_{10}(m/H_G)$ and the H content ($H/H+C = 25 + 9 \log_{10}(m/H_G)$) [4], similarly to what was previously obtained for as-deposited samples for which the H content varied from 20 to 47 at. % [5, 6]. We have emphasized that m/H_G is sensitive not only to the H content, but also to defect passivation [7, 8], possibly by H migration, and we also found that m/H_G is due only to H bonded to $C(sp^3)$. In addition we have obtained a linear relation between H_D/H_G and the H content ($H/H+C = 0.54 - 0.53 H_D/H_G$), independent of whether the H is bonded to $C(sp^2)$ or to $C(sp^3)$. H_D/H_G can thus be used to probe the total H content in the range from 2 to 30 at.%. Conversely, we have shown that the Γ_G and the σ_G parameters are sensitive mainly to the structural changes such as the re-organization leading to a larger aromatization and the loss of $C(sp^3)$ induced by heating.

To obtain more information on the different processes involved under heating we investigate here the long term kinetics of the isothermal hydrogen release from a-C:H films with initial H/H+C ratios of 0.29, 0.32 and 0.37 at temperatures of 450 °C, 500 and 600 °C by means of in situ Raman microscopy. We show how the evolution kinetics provide valuable information on the H release processes and emphasize the role of the initial structure and H-content on these processes.

2. Experimental

Plasma-deposited hydrogenated amorphous carbon films, a-C:H, with H/H+C \sim 0.29, 0.32 and 0.37 (DC self bias of -300, -200 and -100 V, respectively), and a thickness of $e \sim 0.20 \mu m$ (see ref. [9] for details on the deposition method) were studied together with a thicker film with H/H+C = 0.32 (applied substrate bias : -200 V) and a thickness of $e \sim 1 \mu m$ (see ref. [5] for details on the deposition method). The 0.29 and 0.32 films are hard films while the 0.37 film is intermediate between a hard and a soft film [9, 10]. Note that the thick film has a larger $C(sp^3)$ content than the three thin films: this is indicated by its G band position at 1540 cm^{-1} instead of 1522 cm^{-1} for the thin films, their G band widths being similar (see figure 9 in [2]). The samples with the as-deposited films were cut into several pieces, each piece being heated under argon flow in a cell at 1.5 bar with a linear ramp of 150 °C min^{-1} to reach the working temperature. Time zero was taken at the end of the ramp. Temperatures 450, 500 and 600 °C were studied.

Raman spectra were obtained using a Horiba-Jobin-Yvon HR LabRAM apparatus (laser wavelength: $\lambda_L = 514.5 \text{ nm}$, 50X objective, numerical aperture of 0.5 leading to a laser focus diameter of 2.5 μm , resolution $\sim 1 \text{ cm}^{-1}$). The laser power was chosen to have a good signal/noise ratio and/or to prevent damages and three values were tested, 0.01, 0.1 and 1 mW, corresponding to power densities from 2×10^2 to $2 \times 10^4 \text{ J cm}^{-2} \text{ s}^{-1}$. Unless otherwise stated, spectra were recorded in situ at the working temperature. The cell was a commercial LINKAM TS1500, argon was Alphagaz 2 (99.9995% purity, Air Liquid Company). The Raman parameters analyzed were the G band wavenumber, σ_G , the G band full-width at half-maximum, Γ_G , the relative height of the G and D bands, H_D/H_G , and the m/H_G parameter. Heights were measured on the raw data after the linear baseline calculated between 800 and 2000 cm^{-1} (slope m) was subtracted. In that case, H_D was therefore measured at its apparent maximum, except when the D band maximum was not sufficiently well defined (i.e. for the as deposited sample). In the latter case H_D was taken at 1370 cm^{-1} . All these parameters are presented in figure 1.

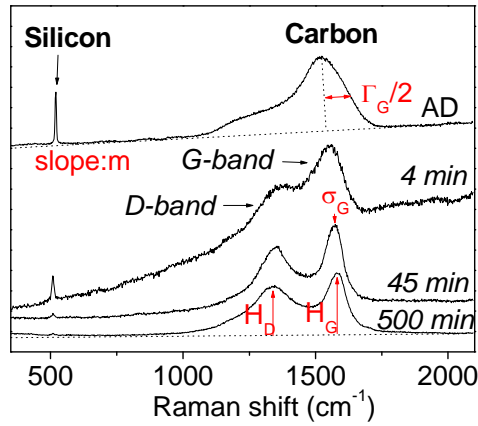


Figure 1: Raman spectra of the a-C:H film ($e = 0.2 \mu\text{m}$ and $H/H+C = 0.32$) at room temperature, as deposited (AD) and at 500 °C after 4, 45 and 500 min at 500 °C.

3. Results and discussion

Figure 1 displays Raman spectra of the a-C:H film ($e = 0.2 \mu\text{m}$, $H/H+C = 0.32$), as deposited at room temperature and after 4, 45 and 500 minutes at 500 °C. The Raman spectrum of the as deposited film is composed of the underlying silicon wafer signature at 520 cm^{-1} , a G band at 1522 cm^{-1} , and a broad shoulder at $\sim 1200 - 1400 \text{ cm}^{-1}$ containing the D band. When the sample is heated, the silicon signature diminishes because the a-C:H becomes more absorbent [11, 12]. The photoluminescence background significantly increases, due to the defect passivation (and the quenching of non-radiative relaxation processes [4, 6]) before it starts decreasing as hydrogen is released. The G band narrows and slightly blueshifts, as previously observed in [4, 13]. The D band also narrows and its height increases. According to previous studies [2, 13, 14], these evolutions reveal the organization of the material, i.e. a loss of $\text{C}(\text{sp}^3)$ and increasing aromatization. When the heating time increases, the Raman spectra keep changing: the G and D bands become more clearly distinguishable, H_D/H_G increases and m/H_G decreases. A long timescale process thus occurs, that we investigate in more detail below.

Figure 2 displays the isothermal evolution with time up to 800 min of σ_G , Γ_G , m/H_G and H_D/H_G at 500 °C at the three laser powers, 0.01, 0.1 and 1 mW for the a-C:H film ($e = 0.2 \mu\text{m}$, $H/H+C = 0.32$). No significant effect of the laser power is observed, indicating that no additional heating due to the laser irradiation is induced even at 1 mW, contrary to what was measured in [15] for thinner (15 nm) films. Figures 2.a and 2.b display a similar isothermal evolution for Γ_G and σ_G , reaching plateaus in ~ 100 minutes. Γ_G is at 180 cm^{-1} for the as-deposited film and the plateau at 500 °C is at 85 cm^{-1} . σ_G is at 1522 cm^{-1} for the as-deposited film and the plateau at 500 °C is at 1580 cm^{-1} . These evolutions suggest that at 500 °C, the film gets rapidly more organized (in typically 100 min) and that this organization then does not significantly evolve. Conversely, figures 2.c and 2.d show that for m/H_G and H_D/H_G this rapid evolution is followed by a slow and roughly linear change (decrease for m/H_G and increase for H_D/H_G). H_D/H_G and m/H_G are both correlated with the H content [4]. We thus interpret these evolutions as due to the isothermal H release, with a first phase occurring rapidly together with structural changes (within about 100 minutes), followed by a second phase occurring on a longer time scale.

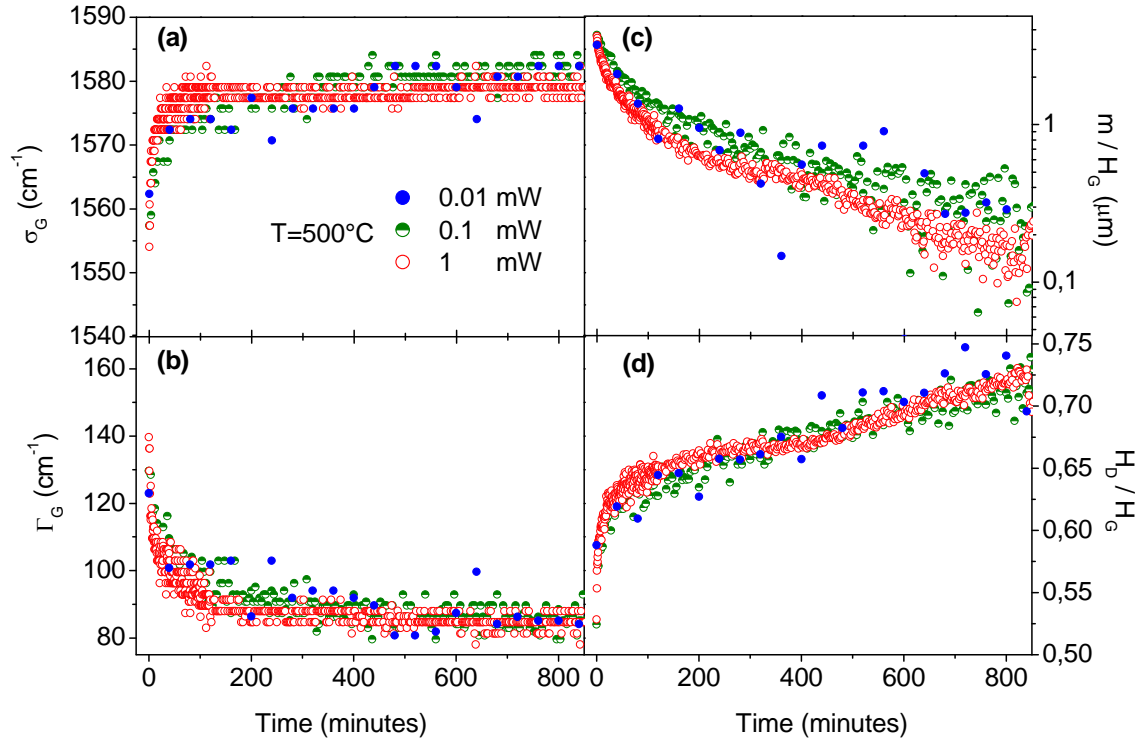


Figure 2: Time evolution of Raman parameters of the $a\text{-C:H}$ film ($e = 0.2 \mu\text{m}$ and $H/H+C = 0.32$) heated at $500 \text{ }^\circ\text{C}$ at three laser powers: (a) G band position, σ_G , (b) G band width, Γ_G , (c) m/H_G parameter, m being the slope of the photoluminescent background and (d) D and G band height ratio, H_D/H_G .

To test the spatial homogeneity of heating-induced changes, we map the film at room temperature after heating at $500 \text{ }^\circ\text{C}$ for 800 min, in a $\sim 35 \times 35 \mu\text{m}^2$ area, much larger than the $5 \mu\text{m}^2$ area of the laser spot, with the 0.01 mW laser power. Histograms obtained by analyzing the maps of the four parameters, σ_G , Γ_G , m/H_G and H_D/H_G are displayed in figure 3. Their widths are small ($\sigma_G = 1601 \pm 2 \text{ cm}^{-1}$, $\Gamma_G = 76 \pm 4 \text{ cm}^{-1}$, $m/H_G = 0.25 \pm 0.09 \mu\text{m}$ and $H_D/H_G = 0.77 \pm 0.02$), indicating that the sample is uniform, both in structure and in composition. The values obtained for Γ_G , m/H_G and H_D/H_G at the end of the 800 min heating at $500 \text{ }^\circ\text{C}$ fall in this range, confirming that the spot irradiated by the laser is not more heated than the other parts of the sample. Conversely, σ_G is at 1580 cm^{-1} at the end of the heating process, significantly outside the histogram values, and this is due to a reversible temperature effect due to multi-phonon interactions, similarly to what was found for graphite or graphene [16]. We have checked that the effect was reversible by varying alternately the temperature between room temperature and $500 \text{ }^\circ\text{C}$.

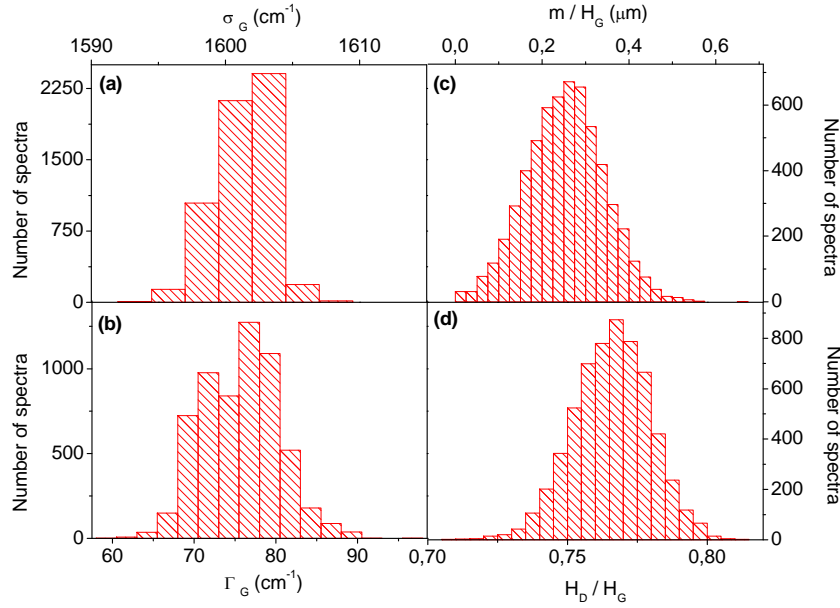


Figure 3: Histograms of the mapping of Raman parameters for the *a*-C:H film of figure 2 at room temperature after 800 minutes at 500 °C. Spectra were recorded on a 35 x 35 μm² area, with a 0.5 μm lateral sampling and a laser power of 0.01 mW. (a) G band position, σ_G , (b) G band width, Γ_G , (c) m/H_G parameter, m being the slope of the photoluminescent background and (d) D and G band height ratio, H_D/H_G .

Figure 4 is a plot similar to that of figure 2 to compare the isothermal evolutions of the three thin films ($\epsilon = 0.2 \mu\text{m}$ and $H/H+C = 0.29, 0.32$ and 0.37) at 500 °C and that of the thick film ($\epsilon = 1 \mu\text{m}$ and $H/H+C = 0.32$) at 450 °C. The laser power was 1 mW, except for the first 400 min at $H/H+C = 0.29$ for which it was only 0.1 mW (as the spot was located at another place on the sample, the small jump in the data is due to the small width of the structure and H-content distribution, see figure 3). For all the Raman parameters at 500 °C and for the first 100 minutes the evolution is the faster the higher the initial H content. This is in agreement with what is known about the stability and the H desorption of this type of hydrogenated films [17-21], the higher the H content, the less stable is the film and the more rapid is the H desorption. For longer times, the plateaus reached by σ_G and Γ_G are almost independent of the initial H content, indicating that the structure of the film at 500 °C is independent of the initial H content. m/H_G goes to zero for the three films at 500 °C while H_D/H_G keeps slowly increasing along three distinct lines. As H_D/H_G depends on to the total H content and $\log_{10}(m/H_G)$ only on H bonded to $C(\text{sp}^3)$, this indicates that at this stage of the kinetics all remaining H is bonded to $C(\text{sp}^2)$. Furthermore, the remaining H content is higher for lower initial H content. The thick film evolution of σ_G and Γ_G and m/H_G at 450 °C is intermediate between the thin films having the H content 0.29 and 0.32 at 500 °C, although the first stage of the kinetics during the first min is faster in the case of the m/H_G and H_D/H_G parameters. The H_D/H_G parameter also indicates that the H becomes significantly lower. This film has a slightly different carbon structure ($C(\text{sp}^3) / C(\text{sp}^2)$ ratio as indicated by the value of the G band position as-deposited film, see experimental section) than the other films but also a different thickness. Note that this type of thick film is known to easily delaminate, which might also play a role on the H-release, this analysis being beyond the scope of this paper. σ_G and Γ_G are known to give similar information [22] and we will use only Γ_G in what follows.

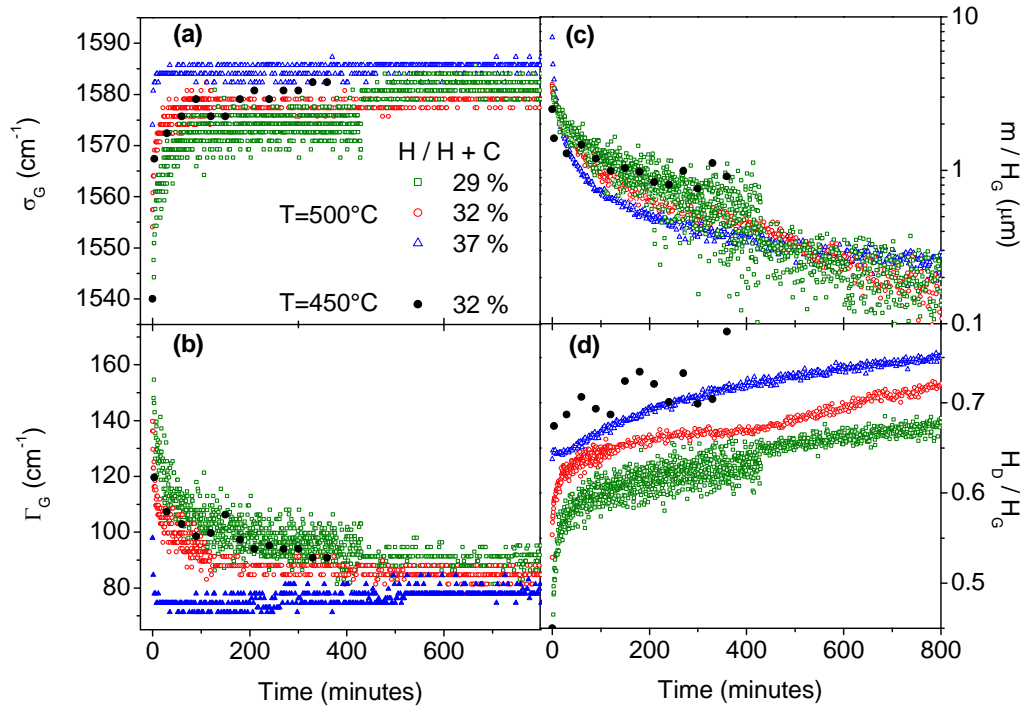


Figure 4: Same as figure 2 for the three thin films ($e = 0.2 \text{ } \mu\text{m}$ and $H/H+C = 0.29, 0.32$ and 0.37) at $500 \text{ } ^\circ\text{C}$ and for the thick film ($e = 1 \text{ mm}$ and $H/H+C = 0.32$) at $450 \text{ } ^\circ\text{C}$.

We now focus on the long term evolutions at different temperatures. Figure 5 displays the isothermal evolution with time up to 6000 minutes of Γ_G , m/H_G and H_D/H_G at 450, 500 and $600 \text{ } ^\circ\text{C}$ for the a-C:H film with $e = 0.2 \text{ } \mu\text{m}$, $H/H+C = 0.29$. As expected, the higher the temperature, the faster the kinetics. A first order exponential law correctly fits the data giving the following estimation of characteristic times: 1370, 140, 2 min for Γ_G , 3340, 190, 4 min for $\log(m/H_G)$, and 2350, 730, 65 min for H_D/H_G , at 450, 500 and $600 \text{ } ^\circ\text{C}$, respectively. The same plateau is found for the three temperatures for Γ_G . This is also the case for m/H_G although the effect is less clear because the signal to noise ratio is significantly lower for the $500 \text{ } ^\circ\text{C}$ data than for the other temperatures. Conversely, the asymptotic value of H_D/H_G increases when the temperature increases. The behaviour of Γ_G suggests that the final stage of organization is the same for all investigated temperatures. More precisely, as Γ_G (as well as σ_G) is related to $C(sp^3)$ defects linked to the aromatic network, it suggests that the vanishing of $C(sp^3)$ defects and the aromatization occur similarly in this temperature range. This is in accordance with X-ray absorption near edge spectroscopy measurements (XANES) reporting that a transition from alkane and non-aromatic carbon sites towards more graphitic environments occurs when heating [21]. m/H_G is also related to $C(sp^3)$, probing H coming only from H bonded to $C(sp^3)$ atoms and consistently, it behaves as Γ_G , going to zero at all temperatures. H_D/H_G probes the full H content, and its different final values suggest that not all the H bonded to $C(sp^2)$ can be released in this temperature range, even with infinite time. Applying the relation between the H content and H_D/H_G (see [4]), the H contents after heating can be estimated at 12 and 8 % at $500 \text{ } ^\circ\text{C}$ and $600 \text{ } ^\circ\text{C}$, respectively. At $450 \text{ } ^\circ\text{C}$, 6000 minutes are not enough to reach a plateau.

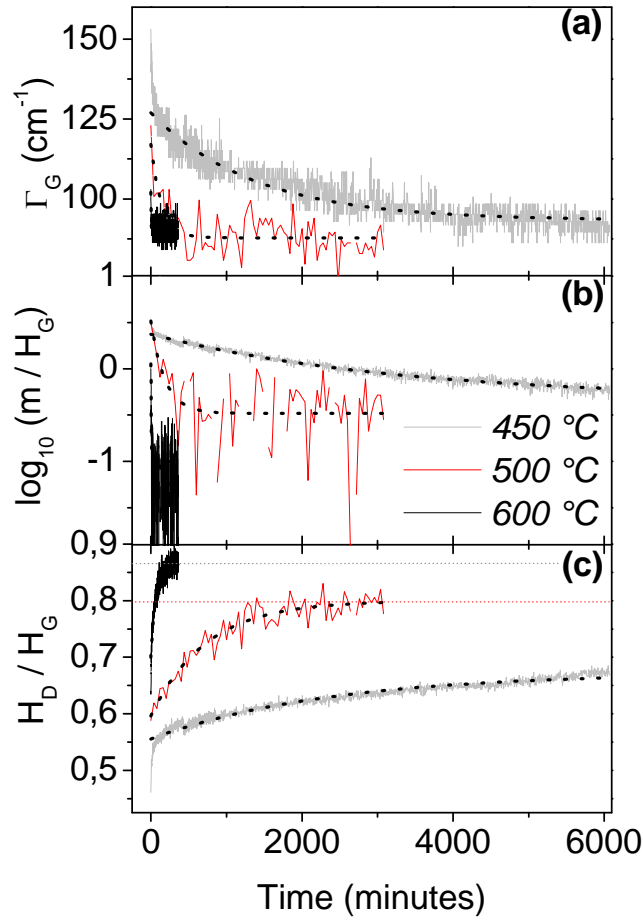


Figure 5: Time evolution of Raman parameters of the $a\text{-C:H}$ film ($e = 0.2 \mu\text{m}$ and $H/H+C = 0.29$) heated at 450, 500 and 600 °C: (a) G band width, Γ_G , (b) m/H_G parameter and (c) D and G band height ratio, H_D/H_G . Black dotted lines are exponential fits.

Even though the understanding of the characteristic times obtained in figure 5 is not straightforward, these times may give information on the processes driving the H release. We have plotted in figure 6 the logarithm of the inverse of these times as a function of the inverse of temperature. The linearity observed indicates that typical activation energies could be deduced, here 2.4 eV for Γ_G and $\log_{10}(m/H_G)$ and 1.3 eV for H_D/H_G . Note that the 2.4 eV activation energy is close to the free activation energy obtained by [23] for the desorption of CH_4 from similar hard layers. The CH_4 formation mechanism is related to the breaking of $\text{C}(\text{sp}^3)\text{-CH}_3$ bonds. This is consistent with our results relating the thermal evolution of Γ_G and $\log_{10}(m/H_G)$ to sp^3 content evolution, and confirms that activation energy of 2.4 eV is typical of sp^3 bond breaking in such materials. A detailed analysis of these observations needs additional data and is beyond the aim of this paper.

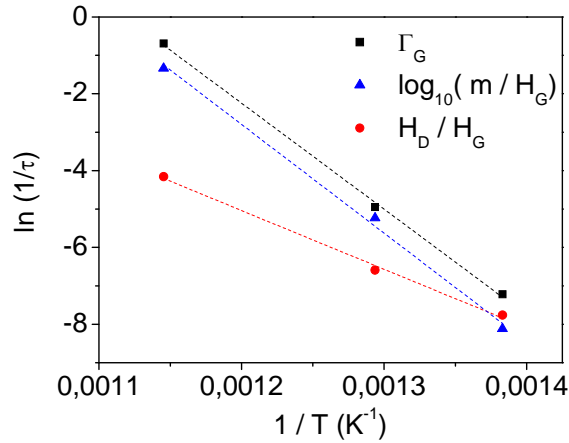


Figure 6. Arrhenius plot of data from the exponential fits of figure 5.

4. Conclusion

The isothermal evolutions of the bonding structure and the H content of a-C:H films from hard to intermediate between hard and soft amorphous carbon, with various H contents ($H/H+C = 0.28, 0.32$ and 0.37) and various thicknesses ($e = 0.2 \mu\text{m}$ and $1 \mu\text{m}$) were studied in the range $450 \text{ }^\circ\text{C} - 600 \text{ }^\circ\text{C}$ by means of Raman microscopy. At $500 \text{ }^\circ\text{C}$, a fast process occurring in less than 100 minutes is evidenced. This is attributed to reorganization of the carbon network, i.e. loss of $C(\text{sp}^3)$ and increasing aromatization. During this reorganization, H begins to be released, the full H release from $C(\text{sp}^3)$ occurring in ~ 15 hours. On longer timescale (~ 50 hours), H keeps being released, but $\sim 12 \%$ of H bonded to $C(\text{sp}^2)$ finally remain. Kinetics is similar, but more (less) rapid, at 600 (450) $^\circ\text{C}$. Kinetics is also faster when the H content is higher, in agreement with what is known on the instability of this type of hydrogenated films when the H content is large. Not only the carbon network organization but also the initial $C(\text{sp}^3)/C(\text{sp}^2)$ ratio can significantly changes the H release kinetics. This type of isothermal kinetics studies reveal information on the processes involved in the H release or in the carbon organization under heating, for example through the determination of activation energies. Additional experiments are currently performed at other temperatures and also with deuterated films to give more data to elucidate these thermally activated processes.

Acknowledgments

We acknowledge the Euratom-CEA association, the EFDA European Task Force on Plasma Wall Interactions, the Fédération de Recherche FR-FCM, the French national research agency ANR (ANR-06-BLAN-0008 contract) and the PACA Region (FORMICAT project) for their financial support. JGB acknowledges the Executive Research Agency of the European Union for funding under the Marie Curie IEF grant number 272448.

References

- [1] F. Tuinstra and J. L. Koenig, *J. Chem. Phys.* 53 (1970) 1126.
- [2] A. C. Ferrari and J. Robertson, *Phys. Rev. B* 61 (2000) 14095.
- [3] J. Schwan, S. Ulrich, V. Bathori, H. Erhardt, and S. R. P. Silva, *J. Appl. Phys.* 80 (1996) 440.
- [4] C. Pardanaud, C. Martin, P. Roubin, G. Giacometti, C. Hopf, T. Schwarz-Selinger, and W. Jacob., *Diamond Relat. Mater.* 34 (2013) 100.
- [5] J. G. Buijnsters, R. Gago, I. Jiménez, M. Camero, F. Agullo-Rueda, and C. Gomez-Aleixandre, *J. Appl. Phys.* 105 (2009) 093510.
- [6] C. Casiraghi, A. C. Ferrari, and J. Robertson, *Phys. Rev. B* 72 (2005) 085401.
- [7] N. M. J. Conway, A. C. Ferrari, A. J. Flewit, J. Robertson, W. I. Milne, A. Tagliaferro, and W. Beyer, *Diamond Relat. Mater.* 9 (2000) 765.
- [8] N. M. J. Conway, A. Ilie, J. Robertson, W. I. Milne, and A. Tagliaferro, *Appl. Phys. Lett.* 73 (1998) 2456.
- [9] T. Schwarz-Selinger, A. von Keudell, and W. Jacob, *J. Appl. Phys.* 86 (1999) 3988.
- [10] C. Hopf, T. Angot, E. Areou, T. Dürbeck, W. Jacob, C. Martin, P. C., P. Roubin, and T. Schwarz-Selinger, (Submitted, 2013)
- [11] C. Pardanaud, E. Areou, C. Martin, R. Ruffe, T. Angot, P. Roubin, C. Hopf, T. Schwarz-Selinger, and W. Jacob, *Diamond Relat. Mater.* 22 (2012) 92.
- [12] T. W. Scharf and I. L. Singer, *Thin Solid Films* 440 (2003) 138.
- [13] A. C. Ferrari and J. Robertson, *Phys. Rev. B* 64 (2001) 075414.
- [14] S. Takabayashi, K. Okamoto, H. Sakaue, T. Takahagi, K. Shimada, and T. Nakatani, *J. Appl. Phys.* 104 (2008) 043512.
- [15] L. H. Zhang, H. Gong, and J. P. Wang, *J. Appl. Phys.* 92 (2002) 2962.
- [16] N. Bonini, M. Lazzeri, N. Marzari, and F. Mauri, *Phys. Rev. Lett.* 99 (2007) 176802.
- [17] C. Wild and P. Koidl, *Appl. Phys. Lett.* 51 (1987) 1506.
- [18] J. Ristein, R. T. Stief, L. Ley, and W. Beyer, *J. Appl. Phys.* 84 (1998) 3836.
- [19] H. Ito, K. Yamamoto, and M. Masuko, *Thin Solid Films* 517 (2008) 1115.
- [20] E. Salançon, T. Dürbeck, T. Schwarz-Selinger, F. Genoese, and W. Jacob, *J. Nucl. Mat.* 376 (2008) 160.
- [21] J. G. Buijnsters, R. Gago, A. Redondo-Cubero, and I. Jimenez, *J. Appl. Phys.* 112 (2012) 093502.
- [22] C. Pardanaud, G. Giacometti, C. Martin, R. Ruffe, T. Angot, E. Areou, B. Pegourie, E. Tsitroni, T. Dittmar, C. Hopf, W. Jacob, T. Schwarz-Selinger, and P. Roubin, *Journal of Nuclear Materials* 415 (2011) S254.
- [23] X. Jiang, W. Beyer, and K. Reichelt, *J. Appl. Phys.* 68 (1990) 1378.